Open access • Journal Article • DOI:10.1109/TPWRS.2019.2942583

Optimal Voltage Control Strategy for Voltage Regulators in Active Unbalanced Distribution Systems Using Multi-Agents — Source link

Ahmed Bedawy, Naoto Yorino, Karar Mahmoud, Yoshifumi Zoka ...+1 more authors

Institutions: Hiroshima University, Aswan University

Published on: 01 Mar 2020 - IEEE Transactions on Power Systems (IEEE)

Topics: Voltage regulation, Voltage regulator, Robust control and Voltage

Bedawy, Ahmed; Yorino, Naoto; Mahmoud, Karar; Zoka, Yoshifumi; Sasaki, Yutaka

Optimal Voltage Control Strategy for Voltage Regulators in Active Unbalanced Distribution Systems Using Multi-Agents

Published in:
IEEE Transactions on Power Systems

DOI:
10.1109/TPWRS.2019.2942583

Published: 01/03/2020

Document Version
Peer reviewed version

Please cite the original version:
Bedawy, A., Yorino, N., Mahmoud, K., Zoka, Y., & Sasaki, Y. (2020). Optimal Voltage Control Strategy for Voltage Regulators in Active Unbalanced Distribution Systems Using Multi-Agents. *IEEE Transactions on Power Systems*, *35*(2), 1023-1035. [8844824]. https://doi.org/10.1109/TPWRS.2019.2942583

Optimal Voltage Control Strategy for Voltage Regulators in Active Unbalanced Distribution Systems Using Multi-Agents

Ahmed Bedawy, *Student Member, IEEE*, Naoto Yorino, *Senior Member, IEEE*, Karar Mahmoud, Yoshifumi Zoka, *Member, IEEE* and Yutaka Sasaki, *Member, IEEE*

***Abstract*— The rapid increase in the installation of renewable energy sources, particularly solar photovoltaic (PV) sources associated with unbalanced features of distribution systems (DS), disturbs the classic control strategy of voltage regulation devices and causes voltage violation problems. This paper proposes an effective control strategy for voltage regulators in the DS based on the voltage sensitivity using a multi-agent system (MAS) architecture. The features of the unbalanced distribution system (UDS) with the PV and different types and configurations of voltage regulators are considered in the proposed strategy. The novelty of the proposed method lies in realizing both the control optimality of minimizing voltage violations and the flexibility to accommodate changes in the DS topology using an MAS scheme. An advantageous feature of using the MAS scheme is the robust control performance in normal operation and against system failure. Simulation studies have been conducted using IEEE 34-node and 123-node distribution test feeders considering high PV penetration and different sun profiles. The results show that the proposed voltage control strategy can optimally and effectively manage the voltage regulators in the UDS, which decrease their operation stresses and minimize the overall voltage deviation.**

***Index Terms*— Distribution system, multi-agents, renewable energy sources, voltage regulation, voltage violation.**

I. Introduction

RECENTLY, the installation of distributed generations (DGs) in distribution systems (DS) has quickly expanded; approximately 178 gigawatts (GW) of renewable power energy has been installed in 2017 worldwide, and 55% of this capacity is generated from solar photovoltaic (PV) sources [1]. This increase can cause serious voltage problems in the DS. The DG installation changes the characteristic of a DS from passive to active, which causes voltage rise, voltage fluctuation and voltage imbalance because of the intermittent and unbalanced PV outputs [2]–[5].

The classic control strategies of the traditional voltage regulation devices, such as the on-load tap changer (OLTC), switchable capacitors (SC) and step voltage regulators (SVRs), are designed based on the unidirectionally power flow scheme from the substation to the loads. The bidirectional power flow caused by the intermittent PV generation can mislead such classic control strategies and cause voltage violations and tap oscillations of the transformers.

Various studies for voltage control have been performed, such as the local coordination techniques [6], [7], optimization techniques [8]–[10], neural network applications [11], [12], and agent-based techniques [13]–[17]. Various strategies have been conducted to mitigate the impact of the high DG penetration on the DS voltage. The approaches can be classified into centralized and distributed methods.

The centralized control methods coordinate voltage regulators by optimizing a certain objective, such as minimizing the voltage deviations and tap operations in DSs. The centralized control scheme is effective for the coordination among the DGs, OLTC, and SC. The approach can include day-ahead coordination [18], [19], management of the DG reactive power [20]–[22], voltage rise mitigation by coordination among battery energy storage systems (BESs) [23]–[26], microgrid voltage regulation [27], [28], and PV inverter reactive power control [29], [30]. These centralized control schemes can realize optimal control, whereas the high performance depends on the cost of the communication system, and its reliability against faults requires continued high investment.

The distributed control scheme relies on the independent decision of distributed controllers, where a coordination method is necessary to address the present voltage problems [31]. This strategy includes the off-line coordination of the parameters of conventional distributed controllers, and a multi-agent system (MAS) scheme that fully utilizes communications among them. There have been various works, such as the charge/discharge of BESs [32], controlling the DG active power generations [33], coordination among the OLTCs, SCs, and PV inverter reactive powers [34]–[36]. The distributed approach is generally more reliable, since the individual controllers can act autonomously, even in the case of faults. However, the optimal performance cannot be achieved in general, except certain cases [37]–[39], where the optimality can be reached when the agents are allowed to communicate and cooperate.

A. Bedawy is with the Graduate School of Engineering, Hiroshima University, 739-8527 Hiroshima, Japan, and also with the Faculty of Engineering, South Valley University, 83523 Qena, Egypt (e-mail: a.bedawy@eng.svu.edu.eg).

N. Yorino, Y. Zoka, and Y. Sasaki are with the Graduate School of Engineering, Hiroshima University, 739-8527 Hiroshima, Japan (e-mail: yorino@hiroshima-u.ac.jp; zo@hiroshima-u.ac.jp; yusasaki@hiroshima-u.ac.jp).

K. Mahmoud is with the Department of Electrical Engineering, Aswan University, 81542 Aswan, Egypt, and also with the Department of Electrical Engineering and Automation, Aalto University, FI-00076 Espoo, Finland (e-mail: karar.alnagar@aswu.edu.eg).

In this paper, an effective voltage control strategy for the voltage regulators in an unbalanced DS (UDS) is proposed by extending the previous studies [40], [13]. The proposed method considers the features of the UDS and different types and configurations of voltage regulators. The difference of the proposed method from the existing methods lies in ensuring an optimal control action to minimize the voltage deviations in a simple manner without using a central controller. Furthermore, it is flexible to handle the possible changes in the DS topology and operations of the PV systems using the distributed MAS scheme. The use of the MAS scheme yields a robust control performance in a flexible and reliable manner, even in the case of agent failure. The proposed method can optimally and effectively manage the voltage regulators in the UDS with an unbalanced PV distribution among the three-phases, decrease the device operation stresses and minimize the total voltage deviation. The proposed method can consider other conventional controllers (e.g., capacitors) to be operated as local controllers with their own setpoints.

The proposed method requires a small improvement in the existing DS devices by installing a blackboard memory and implementing a simple control unit at each voltage regulator. A highly simple communication tool is required in this instance between the blackboard and each local controller in the voltage regulator. In this case, the optimal control among regulators can be realized with a much lower installation cost than the centralized control scheme.

II. Proposed Control Strategy

A. Proposed MAS Control strategy for the UDS

The construction of the DS includes unbalanced loads, unbalances in lines, single-phase or three-phase DG sources, and different configurations of voltage regulation devices. Therefore, a UDS can be represented as an MAS consisting of different agents. Each voltage regulator will act as a control agent that works autonomously according to the data received from the blackboard memory (BM). The BM is used to achieve the optimality of the control objective.

The proposed MAS architecture is illustrated in Fig. 1 for the UDS, and it has the following features:

- Each agent receives information from two sources: measurements from its own area and from the BM.
- Each agent can calculate its own control parameter (referred to as index S in this paper) based on the obtained information.
- The BM collects information from all agents, and each agent recognizes the status of the other agents through this information.
- Each agent takes action according to the received information from the BM to minimize an objective.
- In case of a communication failure, each agent can optimally control itself to achieve its desired goals based on the available data.

A management agent can be useful for system monitoring and real-time calculation, while the proposed method can autonomously work and optimally perform without using it.

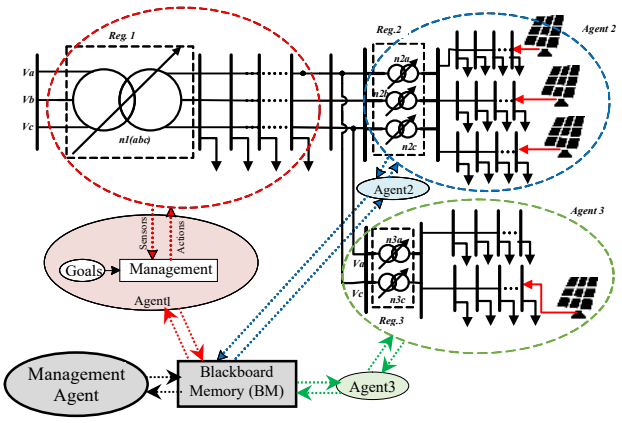

Fig. 1. Proposed MAS for the UDS.

The optimality of the proposed method is explained in the Appendix.

B. Optimal voltage control strategy

The optimality is realized each time by selecting the most effective controller (k) in the set of all discrete control parameters (K) to reduce the absolute value of the total voltage deviations in the system. The objective is to minimize (1).

$$\min_{k\in K} \int_0^{\infty} VD_{abc}(\boldsymbol{v})\,dt, \quad VD_{abc}(\boldsymbol{v}) \geq 0 \tag{1}$$

In this formula, VD_{abc} is the positive three-phase voltage deviation function, which is defined as the sum of the voltage deviations at all observation points in the DS from the reference values. Since UDSs can have different line configurations, including star and delta, the voltage deviation function consists of the voltages in the DS with all line configurations as follows:

$$VD_{abc}(\boldsymbol{v}) = \underbrace{VD_a(\boldsymbol{v}) + VD_b(\boldsymbol{v}) + VD_c(\boldsymbol{v})}_{Yconfig.} + \underbrace{VD_{ab}(\boldsymbol{v}) + VD_{bc}(\boldsymbol{v}) + VD_{ca}(\boldsymbol{v})}_{\Delta config.}$$

$$= \underbrace{\frac{1}{2}\sum_{Y=a}^{c}\sum_{j=1}^{M_Y} w_j^Y.(v_j^Y - v_{Rj}^Y)^2}_{Yconfig.} + \underbrace{\frac{1}{2}\sum_{\Delta=ab}^{ca}\sum_{i=1}^{M_\Delta} w_i^\Delta.(v_i^\Delta - v_{Ri}^Y)^2}_{\Delta config.} \tag{2}$$

For Y-connected regions:

- VD_a, VD_b, and VD_c are the voltage deviation functions for phases a, b, and c, respectively.
- v_j^Y is the voltage at node j phase Y (Y= a, b, c).
- w_j^Y is the weight coefficient of node j phase Y.
- v_R^Y is the reference value of the phase voltage.

For Δ-connected regions:

- VD_{ab}, VD_{bc}, and VD_{ca} are the voltage deviation functions for lines ab, bc, and ca, respectively.
- v_i^Δ is the line voltage at node i, and (Δ= ab, bc, ca).
- w_i^Δ is the weight coefficients of node i line Δ.
- v_R^Δ is the reference value of the line voltage.

The weight coefficients in (2) can be considered indicators of the importance of individual observation points. The constraints of minimization (1) are the power flow equations (3) and those for the tap operations, which will be provided in the next section.

III. CONTROL METHOD FORMULATION

A. Mathematical formulation

The voltages in the UDS are governed by the power flow equations, and they are the function of the tap positions of voltage regulators *n,* and the load parameters *L* are described in (3).

$$\boldsymbol{v} = \boldsymbol{f}\left(\boldsymbol{L},\boldsymbol{n}\right) \tag{3}$$

where, $\boldsymbol{v} = [v_1, v_2,..., v_M]^T$, $\boldsymbol{n} = [n_1, n_2,..., n_N]^T$ and $\boldsymbol{L} = [L_1, L_2,..., L_p]^T$.

Since the proposed method depends on controlling the voltage regulator taps to minimize the overall voltage deviation, the next tap position of regulator *k,* $n_k^p(t+1)$ is a control parameter, which can be expressed as follows:

$$n_k^p(t+1) = n_k^p(t) + \Delta n_k^p(t)\ , \quad n_{k,\min}^p \le n_k^p \le n_{k,\mathrm{m}}^p$$
$$\text{where, } p \in \begin{cases} a,b,c & \text{for Y connected regulators} \\ ab,bc,ca & \text{for } \Delta \text{ connected regulators} \end{cases} \tag{4}$$

The tap change in regulator *k* at time *t* is described by $\Delta n_k^p(t)$, and it depends on the regulator step size and tap status, which can be expressed as follows:

$$\Delta n_k^p(t) = R_k^p \cdot Z_k^p(t), \quad Z_k^p(t) = \begin{Bmatrix} +1 & \textit{(tap increase)} \\ 0 & \textit{(no tap change)} \\ -1 & \textit{(tap decrease)} \end{Bmatrix} \tag{5}$$

where R_k^p and $Z_k^p(t)$ are the step size and tap status of regulator *k* phase or line *p,* respectively.

According to (3), the change in the objective is given as

$$\begin{aligned} \Delta VD_{abc}(\boldsymbol{v}(t)) &= VD_{abc}(\boldsymbol{v}(t+1)) - VD_{abc}(\boldsymbol{v}(t)) \\ &= \left[\frac{\partial VD_{abc}}{\partial \boldsymbol{v}}\right] \cdot \left[\frac{d\boldsymbol{v}}{d\boldsymbol{n}}\right] \cdot\ \Delta\boldsymbol{n}(t) \end{aligned} \tag{6}$$

Equation (6) can be written as follows:

$$\begin{aligned} \Delta VD_{abc}(t) &= \left[\frac{\partial VD_{abc}}{\partial \boldsymbol{v}}\right] \cdot \left[\frac{d\boldsymbol{v}}{d\boldsymbol{n}}\right] \cdot \boldsymbol{R}\ .\ \boldsymbol{Z}(t) \\ &= \boldsymbol{S}_{abc}(t)\ .\ \boldsymbol{Z}(t) = \sum_{k=1}^{N} S_{k(abc)}(t)\ .\ Z_k(t) \\ &= \underbrace{\sum_{y=a}^{c}\sum_{j=1}^{N_y} S_j^y(t)\ .\ Z_j^y(t)}_{Y\mathit{config.}} + \underbrace{\sum_{x=ab}^{ca}\sum_{i=1}^{N_x} S_i^x(t)\ .\ Z_i^x(t)}_{\Delta\mathit{config.}} \end{aligned} \tag{7}$$

where

$\boldsymbol{Z}(t) = [Z_1(t), Z_2(t), ...Z_N(t)]^T$ and $\boldsymbol{R}(t) = diag[R_1(t), R_2(t), ...R_N(t)]$.

$\boldsymbol{S}_{abc}(t)$ is the sensitivity of the objective with respect to the unit change in the regulator taps; therefore, $\boldsymbol{S}_{abc}(t)$ can be used as an index for optimal control to find the most effective controller. The index can be computed as follows:

$$\begin{aligned} \boldsymbol{S}_{abc}(t) &= \left[\frac{\partial VD_{abc}}{\partial \boldsymbol{v}}\right] \cdot \left[\frac{d\boldsymbol{v}}{d\boldsymbol{n}}\right] \cdot \boldsymbol{R} = \underbrace{\sum_{y=a}^{c}\sum_{j=1}^{N_y} S_j^y(t)}_{Y\ \mathrm{Regulators}} + \underbrace{\sum_{x=ab}^{ca}\sum_{i=1}^{N_x} S_i^x(t)}_{\Delta\ \mathrm{Regulators}} \\ &= \left[S_1(t), S_2(t),\ ..., S_N(t)\right]. \end{aligned} \tag{8}$$

where $[d\boldsymbol{v}/d\boldsymbol{n}]$ is the voltage/tap sensitivity matrix calculated by (3). N_y and N_x are the number of phase and line voltage regulators for the star and delta configurations, respectively.

An optimal control to minimize the objective can be realized using the three-phase index *S* as follows.

$$\min_{k\in K}\ VD_{abc}(\boldsymbol{v}(t+1)) = VD_{abc}(\boldsymbol{v}(t)) + \min_{k\in K}\{\boldsymbol{S}_{abc}(t).\boldsymbol{Z}(t)\} \tag{9}$$

− For optimal operation

The proposed strategy can perform an optimal operation for the UDS by calculating only index *S* in each control agent. If the index values are shared among agents, each agent can independently take its control action. According to (9), the agent with the highest value of index *S* should change its regulator taps as follows:

$$\begin{aligned} S_k^p(t) &= \max\left|[S_1^p(t), ..., S_N^p(t)]\right| > \alpha \\ &= \max_i\left|S_i(t)\right| > \alpha \end{aligned} \tag{10}$$

where α is a threshold value, $i \in K = \{1,\ldots, N\}$, and *N* is the number of system regulators.

Tap *k* will change according to

$$\begin{aligned} &\textit{if } \left|S_k^p(t)\right| = \max_{i,p}\left|S_i^p(t)\right| \quad \textit{and } S_i^p(t) < -\alpha \quad \textit{then } Z_k^p(t) = 1 \\ &\textit{if } \left|S_k^p(t)\right| = \max_{i,p}\left|S_i^p(t)\right| \quad \textit{and } S_i^p(t) > \alpha \quad \textit{then } Z_k^p(t) = -1 \\ &\textit{if } \left|S_k^p(t)\right| \ne \max_{i,p}\left|S_i^p(t)\right| \quad \textit{then } Z_k^p(t) = 0 \end{aligned} \tag{11}$$

In the optimal control strategy, each agent should know the index *S* values of the other agents. At each time *t*, the values of the indices are compared, and the controller with the highest value is activated as described in (11). This action ensures that the agents minimize the overall voltage deviation and local voltage deviations of the violated area. The proposed control strategy described in (10) and (11) can be useful even in the conventional centralized control scheme.

− For suboptimal operation

The proposed suboptimal scheme is to avoid the comparison process among the values of indices of the other agents. We propose that each agent performs control by its own index *S* when it is greater than a predefined threshold as below.

$$\begin{aligned} &\textit{if } S_k^p(t) < -\alpha_0 \quad \textit{then } Z_k^p(t) = 1 \\ &\textit{if } S_i^p(t) > \alpha_0 \quad \textit{then } Z_k^p(t) = -1 \\ &\textit{if } \left|S_k^p(t)\right| < \alpha_0 \quad \textit{then } Z_k^p(t) = 0 \end{aligned} \tag{12}$$

where $\underset{\alpha_0 \ne 0}{\alpha_0} \ge \alpha \ge 0$.

Threshold α_0 is a common value among all controllers. This treatment expects that only one controller reacts at a time, which implies the optimal action. The suboptimal control strategy can be used even in the normal condition. In this case, each agent can act independently as a decentralized control system according to (12). This strategy is suitable for autonomous control but does not guarantee strict optimality (See Appendix). The suboptimal strategy is useful when the data from the other agents are not fully available or reliable. If an agent fails to know the index *S* values of other agents because of communication loss or any abnormal conditions, it will act based on its own measurements.

The threshold values (α and α_0) in (11) and (12) are used as tuning factors that determine the amount of voltage deviation that causes the taps to take actions. Therefore, the threshold values (α and α_0) are useful to adjust the response time of the

controllers. A large value admits a large voltage deviation, which implies that the responses of the controllers become slow and vice versa. The threshold value can be set by the system operator.

B. Formula of Index S

Based on (8) and (9), index *S* for regulator *k* is written as

$$S_k^p(t) = r_k^p \cdot \sum_p \sum_{j=1}^{M_{kp}} \frac{VD_{abc}}{\partial v_j^p} \cdot \frac{dv_j^p}{dn_k^p} = r_k^p \cdot \sum_p \sum_{j=1}^{M_{kp}} w_j^p \cdot (v_j^p - v_R) \cdot \frac{dv_j^p}{dn_k^p} \quad (13)$$

where M_{kp} is the number of observation nodes for the area of regulator *k*.

The voltage/tap sensitivity matrix [*dv/dn*] is an important term in the computation of three-phase index *S* as in (13). It is a possible strategy that the accurate real-time calculation of the voltage/tap sensitivity matrix is performed on-line by the management agent based on the power flow computation using (3). In this case, the proposed method is effective for any networks including the meshed configuration. However, to reduce the computational burden of the control process, a simplified method for radial networks is proposed in the next section.

C. Voltage/tap sensitivity matrix formulation

The voltage/tap sensitivity matrix can be approximated based on only the network configuration assuming that all transformers are ideal [40], [41]. The voltage/tap sensitivities for different types of regulators and system configurations are given as follows:

1) Single-phase regulators

The approximate values for the voltage/tap sensitivity matrix for the single-phase regulator are described in (14).

$$\frac{\partial v_{Hk}}{\partial n_k} = 0, \qquad \frac{\partial v_{Gk}}{\partial n_k} = 1 \quad (14)$$

where *G* is the set of system nodes that can be affected by changing tap *k* (downstream nodes), and *H* is the other nodes that are not affected by changing the tap (upstream nodes).

2) Three-phase star connected regulators

The three-phase star connected regulators can be classified into two categories as follows:

a) Three taps ganged together: In this type, the three taps simultaneously change; therefore, they can be modeled as one controller, as described in (15) and (16).

$$n_a = n_b = n_c = n_{k(abc)} \quad (15)$$

The voltage/tap sensitivity matrix is as follows:

$$\frac{dv_{Gk(abc)}}{dn_{k(abc)}} = \begin{pmatrix} \frac{\partial v_{ka}}{\partial n_{k(abc)}} \\ \frac{\partial v_{kb}}{\partial n_{k(abc)}} \\ \frac{\partial v_{kc}}{\partial n_{k(abc)}} \end{pmatrix} = \begin{pmatrix} 1 \\ 1 \\ 1 \end{pmatrix} \quad (16)$$

b) Three independently controlled regulators: In this type, the tap of each phase can change separately, which is modeled as three independent regulators. The voltage/tap sensitivity matrix for this type of regulators is as follows:

$$\frac{\partial v_{Gk(a,b,c)}}{\partial n_{k(a,b,c)}} = \begin{pmatrix} \frac{\partial v_{ka}}{\partial n_{ka}} & \frac{\partial v_{ka}}{\partial n_{kb}} & \frac{\partial v_{ka}}{\partial n_{kc}} \\ \frac{\partial v_{kb}}{\partial n_{ka}} & \frac{\partial v_{kb}}{\partial n_{kb}} & \frac{\partial v_{1b}}{\partial n_{kc}} \\ \frac{\partial v_{kc}}{\partial n_{ka}} & \frac{\partial v_{kc}}{\partial n_{kb}} & \frac{\partial v_{kc}}{\partial n_{kc}} \end{pmatrix} = \begin{pmatrix} 1 & 0 & 0 \\ 0 & 1 & 0 \\ 0 & 0 & 1 \end{pmatrix} \quad (17)$$

where n_{ak}, n_{bk}, n_{ck} are taps a, b and c, respectively, for regulator *k*. The number of independent taps in (17) vary with the existing phases.

3) Delta connected regulators

a) Closed delta: The voltage equations for closed delta regulators in [7] is used to derive the approximated voltage/tap sensitivity matrix as follows:

$$\frac{\partial v_{Gk(ab,bc,ca)}}{\partial n_{k(ab,bc,ca)}} = \begin{pmatrix} \frac{\partial v_{kab}}{\partial n_{kab}} & \frac{\partial v_{kab}}{\partial n_{kbc}} & \frac{\partial v_{kab}}{\partial n_{kca}} \\ \frac{\partial v_{kbc}}{\partial n_{kab}} & \frac{\partial v_{kbc}}{\partial n_{kbc}} & \frac{\partial v_{1bc}}{\partial n_{kca}} \\ \frac{\partial v_{kca}}{\partial n_{kab}} & \frac{\partial v_{kca}}{\partial n_{kbc}} & \frac{\partial v_{kca}}{\partial n_{kca}} \end{pmatrix} = \begin{pmatrix} 1 & 1 & 0 \\ 0 & 1 & 1 \\ 1 & 0 & 1 \end{pmatrix} \quad (18)$$

where n_{kab}, n_{kbc}, n_{kca} are the taps of lines ab, bc, and ca, respectively, for regulator *k*. As observed from (18), the change in a single tap will affect the voltages in two phases.

b) Open delta: In this type of regulator configuration, two single-phase regulators are connected between two phases. The voltage/tap sensitivity matrix for the two single-phase regulators connected between phases *AB* and *CB* is expressed in (19).

$$\frac{\partial v_{Gk(a,b,c)}}{\partial n_{k(a,b,c)}} = \begin{pmatrix} \frac{\partial v_{kab}}{\partial n_{kab}} & \frac{\partial v_{kab}}{\partial n_{kbc}} & \frac{\partial v_{kab}}{\partial n_{kca}} \\ \frac{\partial v_{kbc}}{\partial n_{kab}} & \frac{\partial v_{kbc}}{\partial n_{kbc}} & \frac{\partial v_{1bc}}{\partial n_{kca}} \\ \frac{\partial v_{kca}}{\partial n_{kab}} & \frac{\partial v_{kca}}{\partial n_{kbc}} & \frac{\partial v_{kca}}{\partial n_{kca}} \end{pmatrix} = \begin{pmatrix} 1 & 0 & 0 \\ 0 & 1 & 0 \\ 1 & 1 & 0 \end{pmatrix} \quad (19)$$

D. *Control procedure*

The proposed control algorithm for each agent is illustrated in Fig. 2, which is explained as follows:

1) Agent measurement process.

In this stage, the agent measures the present tap position and voltages of the observation points in its monitoring area.

2) Agent calculation process.

Based on the measurements, the agent will calculate the following parameters:

a) Center voltage: The minimum and maximum voltage values are identified to compute the center voltage as follows.

$$vc_k^p = \frac{v_{k\min}^p + v_{k\max}^p}{2} \quad (20)$$

where $v_{k\min}^p$ and $v_{k\max}^p$ are the minimum and maximum voltages, respectively, at phase or line *p* of area *k* as shown in Fig. 3.

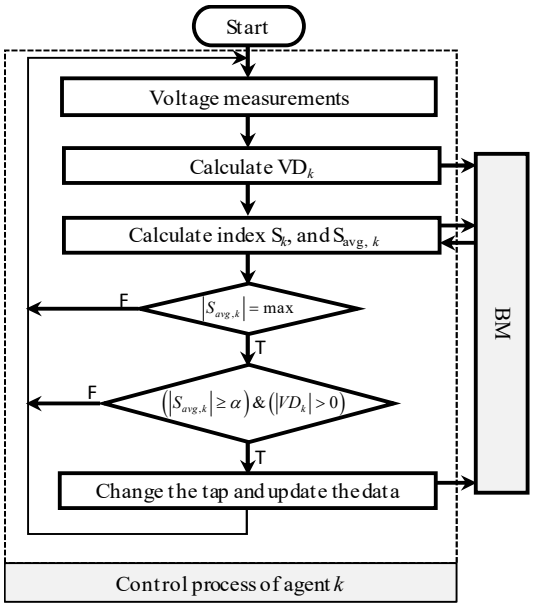

Fig. 2. Proposed voltage control method.

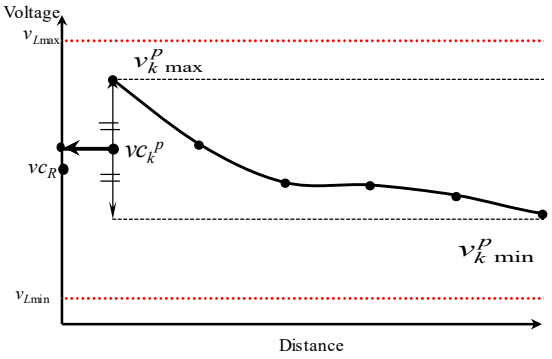

Fig. 3. Utilized voltage control parameters in area k.

b) Voltage deviation: The deviation of the center voltage from its reference value is calculated as follows:

$$VD_k^p = (vc_k^p - \max(d, vm_k^p) - vc_R) \tag{21}$$

$$vm_k^p = \left[\frac{v_{k\,\max}^p - v_{k\,\min}^p}{2}\right] - \left[\frac{v_{L\max} - v_{L\min}}{2}\right] \tag{22}$$

$$vc_R = \frac{v_{L\min} + v_{L\max}}{2} \tag{23}$$

where v_{Lmin} and v_{Lmax} are the standard minimum and maximum voltage limits, and d is a small positive value that acts as a dead band. The dead band (d) is adjusted by the operator based on the system condition and is a function of nominal voltage, where the value is ±1% of the nominal voltage in this study.

c) Index S: Three-phase index S is calculated using (13).

d) Moving average of index S: To ensure a smoothed control action, the time series moving average of index S is calculated using (24).

$$S_{avg,k}^p = \frac{1}{n}\sum_{j=1}^{n} S_k^p \tag{24}$$

3) Agent data collection

The agent sends the voltage deviation of (21) and average values of index S of (24) to the BM. (When the data are accepted by the BM, the BM will classify the status of each agent data as "1" for updated data and "0" for old data).

4) Agent control action:

The agent reads the BM data for the other agents and takes action. The action will differ according to the agent data status as follows:

a) Optimal action: When all agents work normally, the own index S is maximum compared with the others, and the tap is within limits, the agent initiates the control action according to (10) and (11).

b) Suboptimal action: The agent initiates the control action when the tap is within limits and the own index S is greater than the presetting threshold value according to (12). This case is useful under system fault. This situation may be identified from the status of the other agent data.

It is noted that the proposed suboptimal control process can easily be completed by only the individual agents without the interaction of the central management agent, since it avoids the comparison process of the indices. Nevertheless, the optimal control performance is realized as shown in Fig. 13 and the Appendix.

IV. Results and Discussion

In this section, different case studies are conducted to evaluate the overall performance of the proposed control strategy. The maximum and minimum system voltages limits used for the simulation are 1.05 p.u. and 0.95 p.u., respectively. All measurements are equally weighted in (2). Two IEEE test systems are used in this study as follows:

A. IEEE 123-node test feeder

The IEEE 123-node test feeder in Fig. 4 represents the UDS characterized by unbalanced loading and four voltage regulators with different configurations as illustrated in Table I [42]. The feeder is classified into four areas; each area can act as a control agent.

The total daily active and reactive power of loads and PV output (Clear and cloudy day) are shown in Fig. 5. The locations of the PV sources and the system configuration are illustrated in Fig. 4. Four cases are investigated to study different scenarios for the PV and network. The investigation is summarized in Table II. In this study, we use $\alpha = 2.45 \times 10^{-7}$ and $\alpha_0 = 3.5 \times 10^{-7}$ for optimal and suboptimal controls. The simulation results will be discussed below:

1) Case C0: Without control

a) Clear day condition

This case illustrates the voltage problems that occur in different regions of the IEEE 123-node test feeder during the clear day of PV as shown in Fig. 5. As illustrated in Fig. 4 and described in Table I, the system is divided into four regions with different regulator configurations.

Fig. 6 illustrates the maximum voltage deviation in the area of regulator no. 4, where the voltage rise problem occurs in phase (c) feeder during the PV peak time due to high PV penetration. Simultaneously, a voltage drop problem appears in phase (a) between hour 11 and 23; the area of three-phase regulator no. 1 also has a voltage drop problem between hour 17 and 22.

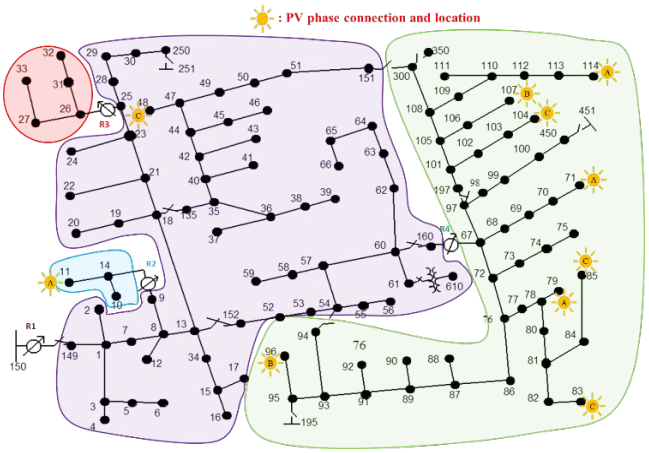

Fig. 4. IEEE 123-node test feeder.

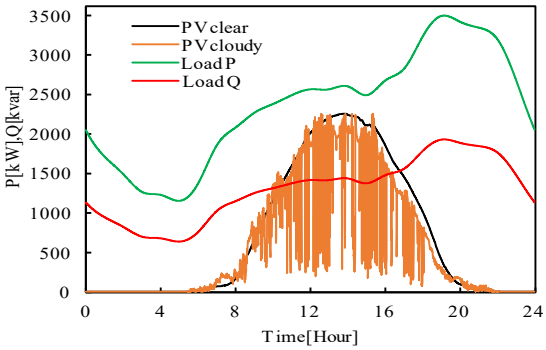

Fig. 5. Total active and reactive power of the loads and PV.

TABLE I
IEEE 123-NODE TEST FEEDER REGULATOR DATA

Reg. ID	Line segment	Phases	Configuration
1	150-149	A-B-C	3-Ph wye, gang operated
2	9-14	A	1-Ph, line-to-neutral connected
3	25-26	A-C	Two 1-Ph, open wye connected
4	160-67	A-B-C	Three 1-Ph, wye connected

TABLE II
TOTAL VOLTAGE DEVIATION AND NO. OF TAP CHANGES

Simulation Cases	Clear day		Cloudy day	
	Total VD	Tap changes	Total VD	Tap changes
C0: Without control	33.20	0	23.10	0
C1: Proposed method (Opt.)	0.012	12	0.124	15
C2: Proposed method (Subopt.)	0.012	12	0.124	15
C3: Proposed (Subopt., failure)	0.012	12	0.132	15
C4: Conventional control	0.242	44	0.505	52
C5: Proposed (Opt., High PV)	0.014	17	0.387	27
C6: Proposed (Subopt., High PV)	0.014	17	0.387	27

b) Cloudy day condition

As shown in Fig. 7 (a), voltage fluctuations with voltage rise and voltage drop problems occur at the peak time of PV power in the area of regulator no. 4 in phases (a) & (c) (nodes 85, 83 and 111). The voltage profile in Fig. 7 (b) illustrates that the area of three-phase regulator no. 1 has a voltage drop problem during hours 17 and 22.

Fig. 7 (b) illustrates the voltage profiles of the nodes at which the large voltage deviations occur; the maximum voltage rise occurs in the area of regulator no. 4 in phase (c) feeder at nodes 83 and 85. The voltage profiles of nodes 65, 111, and 83 show that the maximum voltage drop occurs at phase (a) for the areas of regulators no. 1 and no. 4.

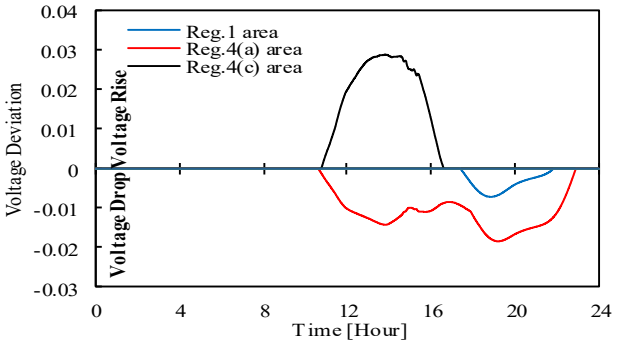

(a) Voltage deviation.

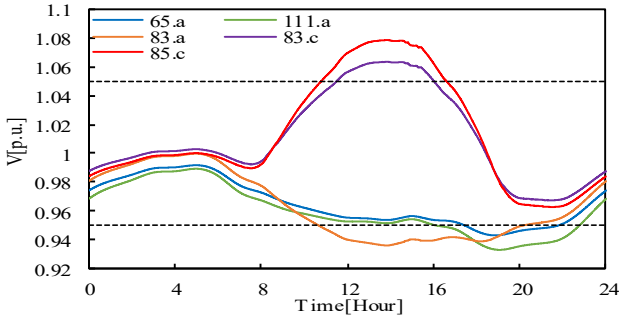

(b) Voltage profiles.

Fig. 6. Results of Case 0: Without control for the clear day.

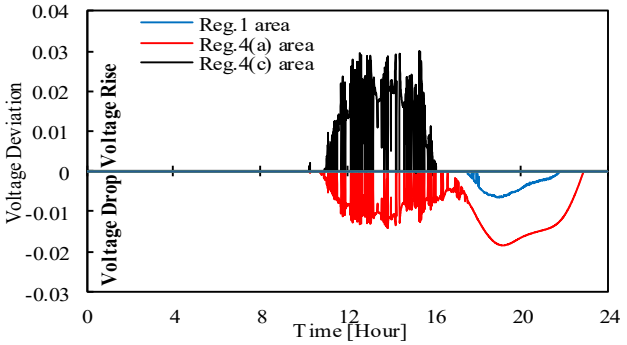

(a) Voltage deviation.

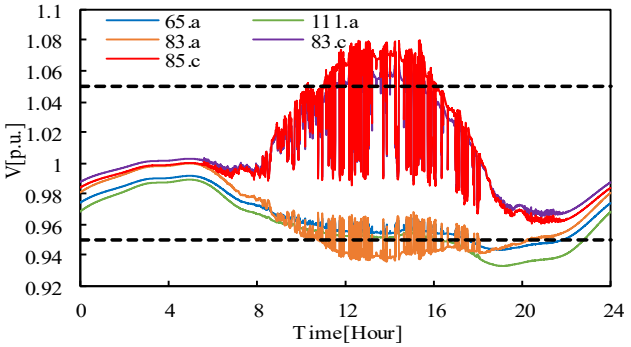

(b) Voltage profiles.

Fig. 7. Results of case 0: Without control for the cloudy day.

2) Case C1: Proposed method (Optimal)

a) Clear day condition

After applying the proposed optimal control strategy, the voltage profiles are improved, where voltage violations are removed as shown in Fig. 8 (a). Fig. 8 (b) illustrates the tap position for each regulator; only three regulators act to mitigate the voltage problems. Based on the proposed control strategy at time t, only the regulator with the most effective ability takes action to mitigate the voltage problems.

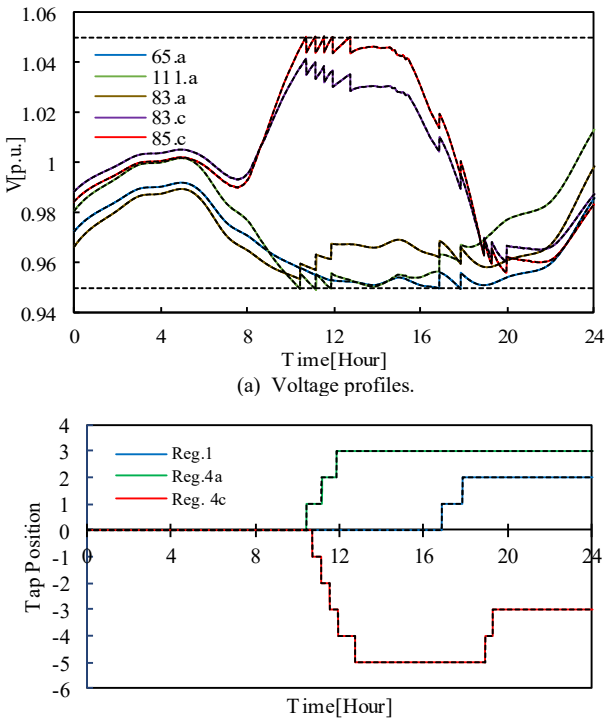

(a) Voltage profiles.

(b) Tap positions.

Fig. 8. Results of the proposed controls for the clear day. (Solid lines: case C1 (Optimal); Dashed lines: case C2 (Suboptimal)).

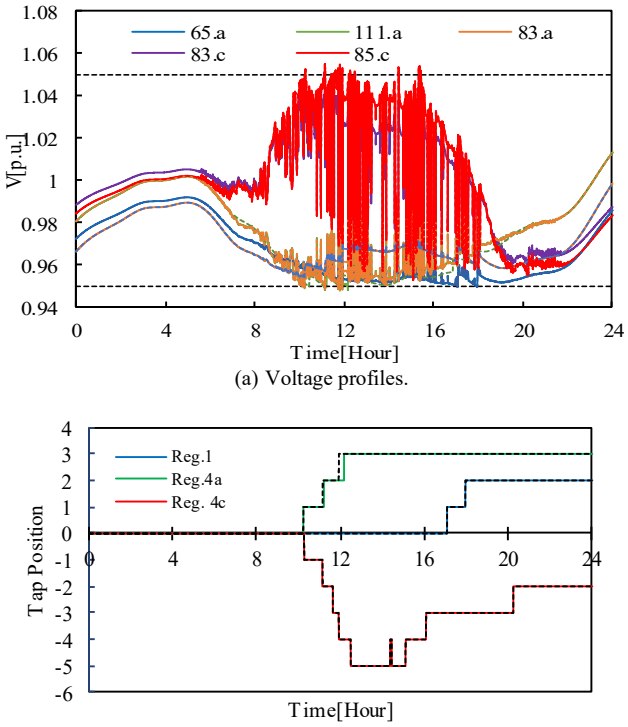

(a) Voltage profiles.

(b) Tap positions.

Fig. 9. Results of the proposed controls for the cloudy day. (Solid lines: case C1 (Optimal); Dashed lines: case C2 (Suboptimal)).

Thus, the proposed method effectively coordinates the tap operations of various voltage regulators, thereby preventing undesirable tap oscillations. The system overall voltage deviation is minimized as illustrated in Table II. Thus, the proposed method can completely solve the voltage violations in the active UDS.

b) Cloudy day condition

A cloudy day of PV generation in Fig. 5 is used to check the performance of the proposed control strategy in the presence of voltage fluctuations. Applying the proposed control strategy to this case clearly mitigates the voltage violation without tap oscillations, as shown in Fig. 9 and Table II. The number of tap changes is slightly increased in the cloudy day compared with the clear day because of the PV output fluctuations. These results show that the proposed optimal control strategy works effectively to reduce the voltage violations without tap oscillations even in the case of PV output fluctuations.

3) Case C2: Proposed method (Suboptimal)

This case represents the proposed suboptimal method in normal condition. As shown in Figs. 8 and 9 and Table II, the performances of the suboptimal method (dashed lines) and the optimal method (solid lines) are almost equivalent. It is noticed from the figures that the regulators react one by one at a different time instant, which implies that the proposed suboptimal law succeeds.

4) Case C3: Proposed method (Suboptimal, Agent failure)

In the case of communication failure among the agents, the performance of the proposed suboptimal method is evaluated. We assume that regulator no. 4 fails to communicate with the BM. The regulator no. 4 agent will act autonomously using only the available data. In this case, since the status of agent no. 4 in the BM has not been updated and is indicated as "0",

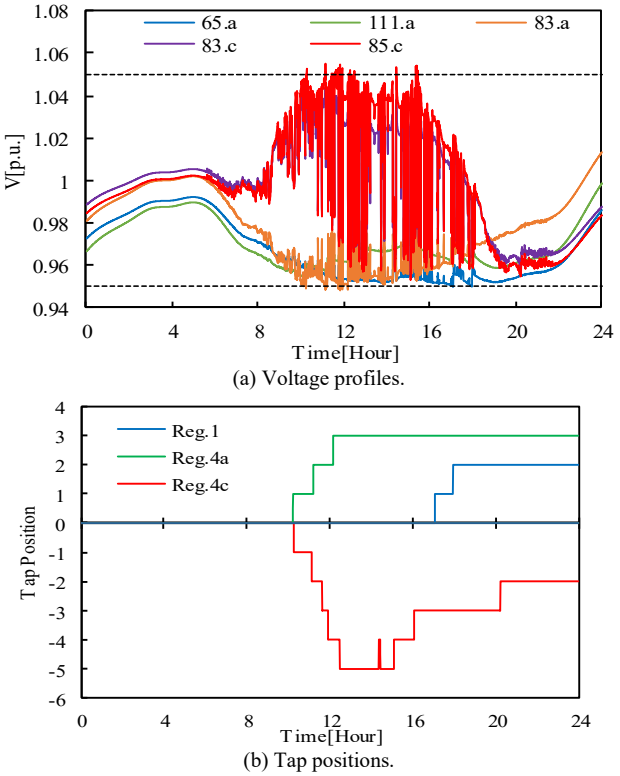

(a) Voltage profiles.

(b) Tap positions.

Fig. 10. Results of case 3: Proposed control for the cloudy day with failure.

the other agents will neglect agent no.4 data and takes their actions to minimize the voltage deviation.

The results for clear and cloudy days are shown in Table II. Both the voltage deviation and number of tap operations are approximately identical to those in the optimal strategy for the clear day. Meanwhile, the voltage deviation is increased

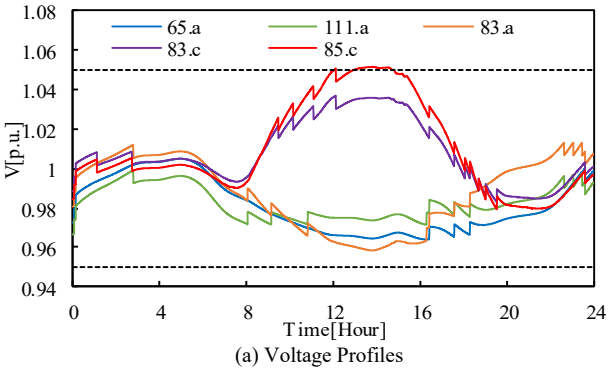

(a) Voltage Profiles

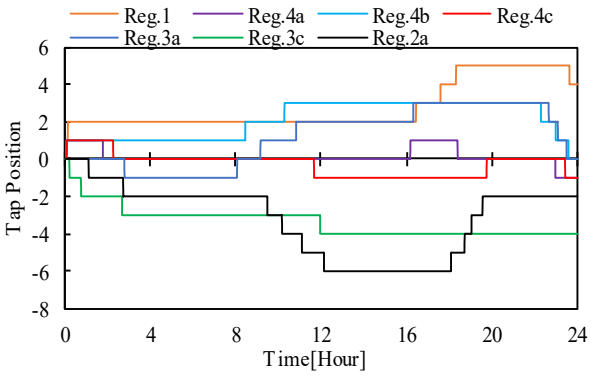

(b) Tap Positions

Fig. 11. Results of case 4: Conventional control for the clear day.

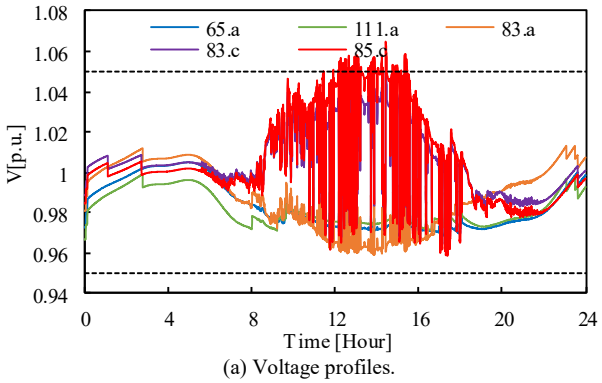

(a) Voltage profiles.

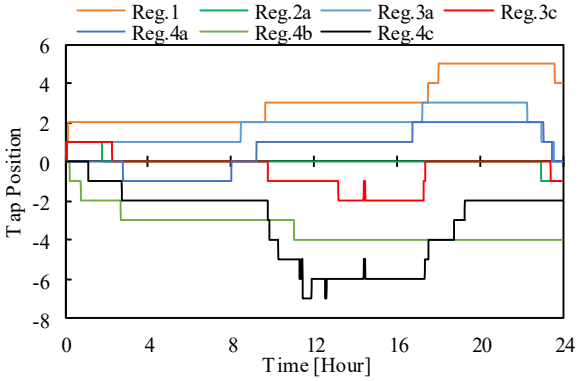

(b) Tap positions.

Fig. 12. Results of case 4: Conventional control for the cloudy day.

for the cloudy day since reg. no.4 works individually based on the suboptimal rule with no cooperation with the other agents as observed in Fig. 10. Thus, the proposed method works effectively even in the case of communication failure.

5) Case C4: Conventional method

Table II lists the performance of a classical control method, which is the line drop compensator approach in [6], [7]. Fig. 11 and Fig. 12 show the voltage profiles and tap operations for clear and cloudy days, respectively. Compared with the conventional method, the proposed method has a high performance in both clear and cloudy days.

6) Cases C5 and C6: Proposed methods (High PV penetration)

In cases C5 and C6, the number of installed PV sources is increased to check the performance of the proposed optimal and suboptimal control strategies, respectively. The results for the clear and cloudy days are shown in Table II. The observed performances are equivalent in both cases, and the number of tap movement is increased compared with Cases 1 and 2 due to the high PV penetration.

7) Overall Performance Evaluations

Fig. 13 shows the performance of the proposed optimal and suboptimal control strategies compared with the conventional control method in the case of the clear day. The total voltage deviations vs. number of tap changes are plotted, where parameters α for optimal and α_0 for suboptimal methods are gradually changed from 0 to $1.1\text{x}10^{-4}$. Each plot is obtained by a 24-hour simulation. The plots of the optimal (circle) and suboptimal (triangle) cases are mostly identical, which implies that the reactions of all regulators (e.g., Figs. 8 and 9) are identical for each 24-hour simulation for different threshold values. Thus, the suboptimal control method can be optimal for a wide range of selected values of α_0. Fig. 13

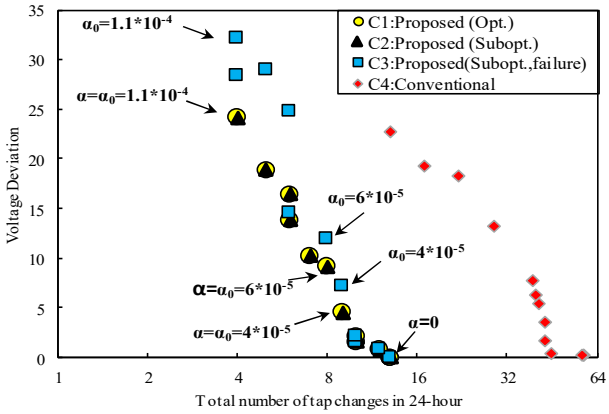

Fig. 13. Voltage deviation vs. tap change in clear day for different α and α_0.

shows that the threshold values α and α_0 are useful to adjust the response time of the controllers. The proposed control system clearly shows a Pareto-optimal characteristic between the number of tap operations and the total voltage deviations.

The performance of the conventional method is also shown in Fig. 13, where the time delay of the line drop compensators is changed as a parameter. Fig. 13 also shows the result for the agent failure for the proposed method. The performance of the proposed method degrades in the case of failure, but it remains acceptable, which is better than the conventional method in normal conditions, since the coordination is performed among the normal agents using the available data.

B. IEEE 34-node test feeder

The IEEE 34-node test feeder is characterized by the unbalanced loading condition with two three-phase star-connected voltage regulators as shown in Fig. 14 [42]. The

proposed control strategy effectively reduces the total voltage deviation with the small number of tap changes compared with the line drop compensator method, as illustrated in the case study of the clear day in Fig. 15 and Table III.

Table III also lists the total computation time to determine the control actions for all agents in each control time. The computational burden of the proposed method to obtain the optimal control is sufficiently fast, but it is greater than the conventional method. Thus, the proposed method can effectively act in real-time circumstances.

V. Conclusions

An effective voltage control strategy is proposed in this paper using an MAS architecture. The objective of the proposed strategy is to optimally minimize the voltage deviation of the UDS under the condition of high PV penetration. The unbalanced features of the DS with different types and configurations of voltage regulators are considered in the formulation. The optimal and suboptimal methods are realized in the proposed voltage control strategy, where each agent can act autonomously based on the available information to minimize the objective. The simulation results show that the proposed strategies can effectively adjust the tap operations to minimize the voltage deviation with no tap oscillations under different sun profiles (sunny or cloudy).

The optimal method requires a comparison process among the indices of the agents, which is more suitable for a centralized control, although it can be applied to an MAS.

The suboptimal method avoids the comparison process among the agents, which can be easily realized by a simple decentralized control strategy using the MAS. The proposed suboptimal method shows an equivalent performance to the optimal method and works reliably even in the case of communication failure. The method can be easily applied to the existing voltage regulators within a reasonable cost of investment compared to a centralized scheme.

As part of the future work, we will upgrade the control algorithm to coordinate with the DG reactive power capability and PV smart inverter functionalities. A hierarchical scheme is under development, where each agent in Fig. 1 will act as a sub-management agent that manages the DGs in its area [43].

VI. Appendix

This appendix explains the optimality of the proposed method from the mathematical viewpoint based on [43]. The equivalent forms to objective functions (1) and (2) are

$$\min\ U(t)=\sum_{t=0}^{\infty} VD_{abc}(\boldsymbol{u}(t)) \tag{A1}$$

$$VD_{abc}(u(t))=\frac{1}{2}\sum_{k=1}^{N} w_k(\boldsymbol{u}_k(t))^2 \tag{A2}$$

In this equation, $\boldsymbol{u}(t)$ is the voltage deviation vector at time t and defined as

$$\boldsymbol{u}(t)=\boldsymbol{g}(\boldsymbol{v}(t))=\boldsymbol{vc}(t)\text{-}\boldsymbol{vc}_R \tag{A3}$$

where, $\boldsymbol{u}(t)=[u_1(t), u_2(t),..., u_N(t)]^T$,
$\boldsymbol{vc}=[vc_1, vc_2,..., vc_N]$ vector of center voltages defined in (20).

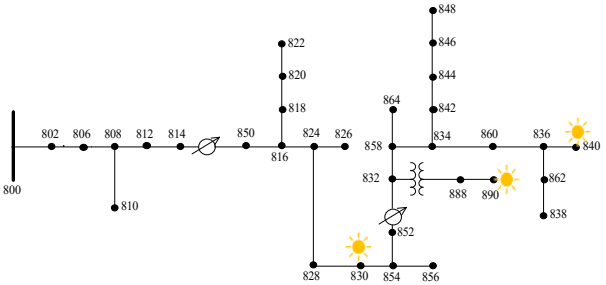

Fig. 14. IEEE 34-node test feeder.

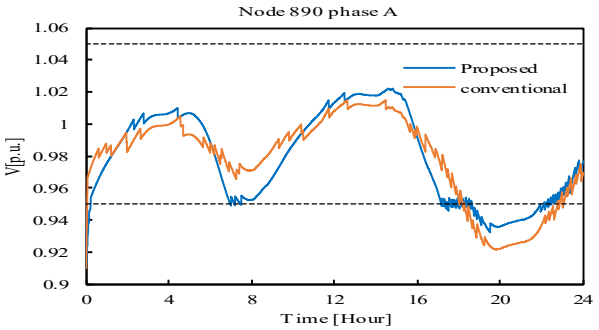

Fig. 15. Voltage profile of node 890 (phase A).

TABLE III
RESULTS OF THE IEEE 34-NODE TEST FEEDER.

	Total VD	Tap changes	computation time (sec/step)
Proposed method	3.51	122	0.00210
Conventional control	14.01	165	0.00031

$\boldsymbol{vc}_R=[vc_{R1}, vc_{R2},..., vc_{RN}]$ vector of target center voltages.

(A2) becomes minimal in the neighborhood of $\boldsymbol{u}=\boldsymbol{0}$, which is referred to as the Equilibrium area in this paper and expressed as follows:

$$E=\{u_1,u_2,\cdots,u_N \mid |u_k|<\varepsilon_k, k=1,\cdots,N\} \tag{A4}$$

with ε_k : dead band of tap k.

Then, we set another objective defined as

$$\min\ \ T,\ \ \boldsymbol{u}(T)\in E \tag{A5}$$

T: number of tap operations to reach the equilibrium from $t=0$.

The voltages in UDS are governed by the power flow equations, and they are the function of tap positions of voltage regulators n and load parameters L, as described in (3).

$$\boldsymbol{v}=\boldsymbol{f}(\boldsymbol{L},\boldsymbol{n}) \tag{3}$$

The linearization of (3) with $v(t)$ at time t around the target voltage with tap control $\boldsymbol{Z}(v(t))$ and load disturbance $\Delta\mathbf{L}(t)$ yields

$$\mathbf{u}(t+1)=\mathbf{u}(t)+\tilde{\mathbf{A}}(t)\cdot\boldsymbol{Z}(t)+\mathbf{B}(t)\cdot\Delta\mathbf{L}(t) \tag{A6}$$

where

$$\tilde{\mathbf{A}}(t)=\mathbf{A}(t)\cdot\mathbf{R},\ \mathbf{A}(t)=[a_{ij}]=[\frac{\partial g}{\partial v}\cdot\frac{\partial v}{\partial n}]_{\substack{n=n(t)\\L=L(t)}}\in{}^{N\times N},$$

$$\mathbf{B}(t)=[\partial v/\partial L]_{\substack{n=n(t)\\L=L(t)}}\in{}^{N\times P},\ \ \Delta\boldsymbol{L}(t)=\boldsymbol{L}(t+1)-\boldsymbol{L}(t),$$

$$\boldsymbol{Z}(t)=R^{-1}\Delta n(t)=R^{-1}(n(t+1)-n(t))=[Z_1(t),Z_2(t),....Z_N(t)]^T$$

$\boldsymbol{R}=diag\ [r_1, r_2,..., r_N]$: regulator step size.

Equation (A2) represents a dynamic system with disturbance

$\Delta \boldsymbol{L}(t)$ and control $\boldsymbol{Z}(t)$. Then, we find the optimal control $\boldsymbol{Z}(t)$ under the following assumptions.

a) At each time *t*, only one tap can act, i.e., only one component of $\boldsymbol{Z}(t) = [Z_1(t), Z_2(t), ...Z_N(t)]$ is "+1" or "-1", and the others are "0" (see (5)).
b) Linearization errors are neglected in the control problem (A1)-(A6).
c) The initial voltage deviation $\boldsymbol{u}$ (0) is $\boldsymbol{u}^0$ ($\boldsymbol{u}$ (0) = $\boldsymbol{u}^0$).
d) Future load disturbances are unknown, which are treated as $\Delta \mathbf{L}(\tau) = 0$, $\tau = t, t+1, \cdots$.

Minimization of the voltage deviations (A1)

The change in (A2) at time *t* is described as follows:

$$\Delta VD_{abc}(\boldsymbol{u}(t)) = VD_{abc}(\boldsymbol{u}(t+1)) - VD_{abc}(\boldsymbol{u}(t)) \tag{A7}$$

If the control is executed to satisfy $\Delta VD_{abc}(t) < 0$, VD_{abc} satisfies the condition of Lyapunov function for the dynamic system. According to the Lyapunov stability criterion, the asymptotic stability of the system (A6) is guaranteed. Therefore, if there is an equilibrium point, the system converges to the equilibrium area E within the finite step T:

$$u(t) = u^e \in E, \quad t \geq T \tag{A8}$$

If there is no equilibrium point, the system converges to a certain point that minimizes VD_{abc}.

Now, Lyapunov function at time T, (A2), is expressed as follows:

$$VD_{abc}(T) = \sum_{\tau=0}^{T-1} \Delta VD_{abc}(\tau) + VD_{abc}(0) = 0 \tag{A9}$$

Assuming that $u^e \approx 0$ due to (A8) at $t=T$,

$$\begin{aligned} U &= \sum_{t=0}^{T} VD_{abc}(t) \\ &= (T+1)\cdot VD_{abc}(0) + T\cdot \Delta VD_{abc}(0) + (T-1)\cdot \Delta VD_{abc}(1) + \\ &\quad \cdots + \Delta VD_{abc}(T-1) \\ &= (T+1)\cdot VD_{abc}(0) + \sum_{t=0}^{T-1} (T-t)\cdot \Delta VD_{abc}(t) \end{aligned} \tag{A10}$$

In (A10), the first term of the right-hand side is constant, and the others are the sum of positively weighted (1, 2,..., *T*) terms. Minimizing each term by the descending order of weight coefficients (*T+1, T...*) will minimize the overall VD_{abc}. The condition to minimize *U* is as follows:

$$\Delta VD_{abc}(0) < \Delta VD_{abc}(1) < \Delta VD_{abc}(T-1) < 0 \tag{A11}$$

This condition is equivalent to the following minimization at each time *t*:

$$\min \quad \Delta VD_{abc}(t) \quad t = 0, 1, 2, ... \tag{A12}$$

Minimization of tap operations (A5)

Assuming the initial tap position $\boldsymbol{n}$ (0) = $\boldsymbol{n}^0$ and equilibrium point position $\boldsymbol{n}(T)$ = $\boldsymbol{n}^e$, the number of tap changes required to the equilibrium point is

$$\boldsymbol{K}^e = R^{-1}(\boldsymbol{n}^0 - \boldsymbol{n}^e) \tag{A13}$$

In this equation, $\boldsymbol{K}^e$ is a vector whose components are integers K_i^e. In other words, K_i^e corresponds to the minimum number of necessary tap changes of each tap *i* to reach the equilibrium point. Therefore, the minimum of tap changes *T* is given by

$$T \geq \left\| \boldsymbol{K}^e \right\|_1 = \sum_{i=1}^{N} \left| K_i^e \right| \tag{A14}$$

The minimum step $\left\| \boldsymbol{K}^e \right\|_1$ can be determined if $\boldsymbol{n}^0$ and $\boldsymbol{n}^e$ are given. To reach the equilibrium within the above minimum steps, the norm of (A15) must be reduced by one step at each time *t* to satisfy (A16).

$$\boldsymbol{K}(t) = R^{-1}(\boldsymbol{n}(t) - \boldsymbol{n}^e) \tag{A15}$$

$$\left\| \Delta \boldsymbol{K}(t) \right\|_1 = \left\| \boldsymbol{K}(t+1) \right\|_1 - \left\| \boldsymbol{K}(t) \right\|_1 \leq -1 < 0 \tag{A16}$$

(A16) implies that $\boldsymbol{n}(t)$ reaches $\boldsymbol{n}^e$ with the minimum step if it is controlled step by step toward $\boldsymbol{n}^e$. Therefore, the control to minimize (A1) also satisfies (A16) and (A5). Note that the conditions for oscillatory action have been analyzed in [44], where (A5) and (A16) are violated.

Control rule

Now, substituting (A6) into (A1), we obtain

$$\begin{aligned} \Delta VD_{abc}(\mathbf{u}(t)) &= VD_{abc}(\mathbf{u}(t+1)) - VD_{abc}(\mathbf{u}(t)) \\ &= \boldsymbol{S}_{abc}(\mathbf{u}(t))\cdot \mathbf{Z}(t) + \mathbf{Z}(t)^T \cdot \mathbf{C} \cdot \mathbf{Z}(t) \\ &= \sum_i (S_{abci}(u)\cdot Z_i + Z \cdot |C_{ii}| \cdot |Z_i|) \\ &\approx \sum_i S_{abci}(u)\cdot Z_i \end{aligned} \tag{A17}$$

where

$$\begin{aligned} &\boldsymbol{S}_{abc}(\mathbf{u}(t)) = \mathbf{u}(t)^T \cdot \mathbf{M} \cdot \tilde{\mathbf{A}}(t), \\ &\mathbf{C} = \tilde{\mathbf{A}}(t)^T \cdot \mathbf{M} \cdot \tilde{\mathbf{A}}(t) \end{aligned} \tag{A18}$$

In this equation, since $C_{ii} \approx 0$ has been numerically confirmed, (A17) holds. Then, the optimal control rule of (9) is obtained. Thus, (A12) is minimized as follows:

Optimal Control Rule

When there is voltage violation at time *t*, a controller that minimizes $\Delta VD_{abc}(t)$ is selected. In other words, at each time *t*, we select at most one controller *k* that satisfies (A19).

$$s_k(u) = \max_i |s_i(u)| > \alpha \tag{A19}$$

with α: threshold value.

This control rule provides the order of controller actions to minimize the objective function.

Suboptimal Control Rule

A simple autonomous control rule is given as follows:

At each time *t*, the controller that satisfies (A20) is activated.

$$\begin{aligned} &u_k(t) > \varepsilon_k \text{ AND } s_k(u_e(t)) > \alpha_0 \text{ [Up]} \\ &u_k(t) < -\varepsilon_k \text{ AND } s_k(u_e(t)) < -\alpha_0 \text{ [Down]} \end{aligned} \tag{A20}$$

According to this rule, each controller can act independently based on its own index *S* and threshold value α_0. The suboptimal control does not provide strict optimality, since in rare cases, it simultaneously allows multiple controls, which may change the optimal sequence of controls given by (A19).

REFERENCES

[1] REN 21, *Renewables 2017: global status report*. 2017.
[2] R. A. Walling, R. Saint, R. C. Dugan, J. Burke, and L. A. Kojovic,

"Summary of Distributed Resources Impact on Power Delivery Systems," *IEEE Trans. Power Deliv.*, vol. 23, no. 3, pp. 1636–1644, Jul. 2008.

[3] N. Mahmud and A. Zahedi, "Review of control strategies for voltage regulation of the smart distribution network with high penetration of renewable distributed generation," *Renew. Sustain. Energy Rev.*, vol. 64, no. March, pp. 582–595, 2016.

[4] D. Santos-Martin, S. Lemon, J. D. Watson, A. R. Wood, A. J. V. Miller, and N. R. Watson, "Impact of solar photovoltaics on the low-voltage distribution network in New Zealand," *IET Gener. Transm. Distrib.*, vol. 10, no. 1, pp. 1–9, 2016.

[5] R. Tonkoski, D. Turcotte, and T. H. M. El-Fouly, "Impact of high PV penetration on voltage profiles in residential neighborhoods," *IEEE Trans. Sustain. Energy*, vol. 3, no. 3, pp. 518–527, 2012.

[6] W. H. Kersting, "Distribution feeder voltage regulation control," *IEEE Trans. Ind. Appl.*, vol. 46, no. 2, pp. 620–626, May 2010.

[7] W. H. Kersting, *Distribution system modelling and analysis*. 2002.

[8] B. A. Robbins, S. Member, and A. D. Domínguez-garcía, "Optimal Reactive Power Dispatch for Voltage Regulation in Unbalanced Distribution Systems," pp. 1–11, 2016.

[9] J. R. Castro, M. Saad, S. Lefebvre, D. Asber, and L. Lenoir, "Optimal voltage control in distribution network in the presence of DGs," *Int. J. Electr. Power Energy Syst.*, vol. 78, pp. 239–247, 2016.

[10] T. S. Vítor, S. Member, and J. C. M. Vieira, "Optimal Voltage Regulation in Distribution Systems With Unbalanced Loads and Distributed Generation," 2016, pp. 1–6.

[11] Z. G.; D. T. Rizy, "Neural Network For Combined Control of Capacitor Banks and Voltage Regulators in Distribution System 00544277.pdf."

[12] Yuan-Yih Hsu and Feng-Chang Lu, "A combined artificial neural network-fuzzy dynamic programming approach to reactive power/voltage control in a distribution substation," *IEEE Trans. Power Syst.*, vol. 13, no. 4, pp. 1265–1271, 1998.

[13] A. Bedawy, N. Yorino, and K. Mahmoud, "Optimal decentralized voltage control in unbalanced distribution networks with high PV penetration," in *2017 Nineteenth International Middle East Power Systems Conference (MEPCON)*, 2017, pp. 1373–1377.

[14] A. Elmitwally, M. Elsaid, M. Elgamal, and Z. Chen, "A Fuzzy-Multiagent Self-Healing Scheme for a Distribution System with Distributed Generations," *IEEE Trans. Power Syst.*, vol. 30, no. 5, pp. 2612–2622, 2015.

[15] Y. Zoka *et al.*, "An effective method for distributed voltage control on system reconfiguration and improper motion of voltage control devices for distribution networks," *IEEJ Trans. Power Energy*, vol. 138, no. 1, pp. 14–22, 2018.

[16] H. E. Z. Farag and E. F. El-Saadany, "A novel cooperative protocol for distributed voltage control in active distribution systems," *IEEE Trans. Power Syst.*, vol. 28, no. 4, pp. 1645–1656, 2013.

[17] F. Ren, M. Zhang, and D. Sutanto, "A multi-agent solution to distribution system management by considering distributed generators," *IEEE Trans. Power Syst.*, vol. 28, no. 2, pp. 1442–1451, 2013.

[18] Y. Kim, S. Ahn, P. Hwang, and S. Member, "Coordinated Control of a DG and Voltage Control Devices Using a Dynamic Programming Algorithm," vol. 28, no. 1, pp. 42–51, 2013.

[19] A. Majumdar, Y. P. Agalgaonkar, B. C. Pal, and R. Gottschalg, "Centralized Volt–Var Optimization Strategy Considering Malicious Attack on Distributed Energy Resources Control," *IEEE Trans. Sustain. Energy*, vol. 9, no. 1, pp. 148–156, Jan. 2018.

[20] S. Deshmukh, B. Natarajan, and A. Pahwa, "Voltage/VAR control in distribution networks via reactive power injection through distributed generators," *IEEE Trans. Smart Grid*, vol. 3, no. 3, pp. 1226–1234, 2012.

[21] A. Abessi, V. Vahidinasab, and M. S. Ghazizadeh, "Centralized support distributed voltage control by using end-users as reactive power support," *IEEE Trans. Smart Grid*, vol. 7, no. 1, pp. 178–188, Jan. 2016.

[22] H. S. Bidgoli and T. Van Cutsem, "Combined Local and Centralized Voltage Control in Active Distribution Networks," *IEEE Trans. Power Syst.*, vol. 33, no. 2, pp. 1374–1384, 2018.

[23] L. Wang, D. H. Liang, A. F. Crossland, P. C. Taylor, D. Jones, and N. S. Wade, "Coordination of Multiple Energy Storage Units in a Low-Voltage Distribution Network," *IEEE Trans. Smart Grid*, vol. 6, no. 6, pp. 2906–2918, Nov. 2015.

[24] S. Gupta, V. Kekatos, and W. Saad, "Optimal Real-Time Coordination of Energy Storage Units as a Voltage-Constrained Game," *IEEE Trans. Smart Grid*, pp. 1–1, 2018.

[25] J. Krata and T. K. Saha, "Real-Time Coordinated Voltage Support with Battery Energy Storage in a Distribution Grid Equipped with Medium-Scale PV Generation," *IEEE Trans. Smart Grid*, pp. 1–1, 2018.

[26] L. Wang, F. Bai, R. Yan, and T. K. Saha, "Real-Time Coordinated Voltage Control of PV Inverters and Energy Storage for Weak Networks with High PV Penetration," *IEEE Trans. Power Syst.*, vol. 33, no. 3, pp. 3383–3395, May 2018.

[27] H. Zhao, M. Hong, W. Lin, and K. A. Loparo, "Voltage and Frequency Regulation of Microgrid With Battery Energy Storage Systems," *IEEE Trans. Smart Grid*, pp. 1–1, 2017.

[28] X. Yang, Y. Du, J. Su, L. Chang, Y. Shi, and J. Lai, "An Optimal Secondary Voltage Control Strategy for an Islanded Multibus Microgrid," *IEEE J. Emerg. Sel. Top. Power Electron.*, vol. 4, no. 4, pp. 1236–1246, Dec. 2016.

[29] T. Ding, C. Li, Y. Yang, J. Jiang, Z. Bie, and F. Blaabjerg, "A Two-Stage Robust Optimization for Centralized-Optimal Dispatch of Photovoltaic Inverters in Active Distribution Networks," *IEEE Trans. Sustain. Energy*, vol. 8, no. 2, pp. 744–754, Apr. 2017.

[30] C. Wu, G. Hug, and S. Kar, "Smart Inverter for Voltage Regulation: Physical and Market Implementation," *IEEE Trans. Power Syst.*, pp. 1–1, 2018.

[31] M. H. Cintuglu, T. Youssef, and O. A. Mohammed, "Development and Application of a Real-Time Testbed for Multiagent System Interoperability: A Case Study on Hierarchical Microgrid Control," *IEEE Trans. Smart Grid*, vol. PP, no. 99, pp. 1–1, 2016.

[32] M. Zeraati, M. E. Hamedani Golshan, and J. Guerrero, "Distributed Control of Battery Energy Storage Systems for Voltage Regulation in Distribution Networks with High PV Penetration," *IEEE Trans. Smart Grid*, vol. 3053, no. c, pp. 1–1, 2016.

[33] P. M. S. Carvalho, P. F. Correia, and L. a F. Ferreira, "Distributed Reactive Power Generation Control for Voltage Rise Mitigation in Distribution Networks," *IEEE Trans. Power Syst.*, vol. 23, no. 2, pp. 766–772, 2008.

[34] P. Jahangiri and D. C. Aliprantis, "Distributed Volt/VAr control by PV inverters," *IEEE Trans. Power Syst.*, vol. 28, no. 3, pp. 3429–3439, 2013.

[35] G. Cavraro and R. Carli, "Local and Distributed Voltage Control Algorithms in Distribution Networks," *IEEE Trans. Power Syst.*, vol. 33, no. 2, pp. 1420–1430, Mar. 2018.

[36] M. Chamana, B. H. Chowdhury, and F. Jahanbakhsh, "Distributed Control of Voltage Regulating Devices in the Presence of High PV Penetration to Mitigate Ramp-Rate Issues," *IEEE Trans. Smart Grid*, vol. 9, no. 2, pp. 1086–1095, Mar. 2018.

[37] E. Dall'anese, H. Zhu, and G. B. Giannakis, "Distributed Optimal Power Flow for Smart Microgrids," *IEEE Trans. Smart Grid*, vol. 4, no. 3, 2013.

[38] S. Bolognani, R. Carli, G. Cavraro, and S. Zampieri, "Distributed Reactive Power Feedback Control for Voltage Regulation and Loss Minimization," *IEEE Trans. Automat. Contr.*, vol. 60, no. 4, pp. 966–981, 2015.

[39] B. Zhang, A. Y. S. Lam, A. D. Dominguez-Garcia, and D. Tse, "An Optimal and Distributed Method for Voltage Regulation in Power Distribution Systems," *IEEE Trans. Power Syst.*, vol. 30, no. 4, pp. 1714–1726, Jul. 2015.

[40] N. Yorino, Y. Zoka, M. Watanabe, and T. Kurushima, "An Optimal Autonomous Decentralized Control Method for Voltage Control Devices by Using a Multi-Agent System," *IEEE Trans. Power Syst.*, vol. 30, no. 5, pp. 2225–2233, Sep. 2015.

[41] A. Bedawy, N. Yorino, and K. Mahmoud, "Management of voltage regulators in unbalanced distribution networks using voltage/tap sensitivity analysis," in *2018 International Conference on Innovative Trends in Computer Engineering (ITCE)*, 2018, pp. 363–367.

[42] "Distribution Test Feeders - Distribution Test Feeder Working Group - IEEE PES Distribution System Analysis Subcommittee." [Online]. Available: https://ewh.ieee.org/soc/pes/dsacom/testfeeders/. [Accessed: 10-Nov-2017].

[43] N. Yorino, T. Watakabe, Y. Nakamura, Y. Sasaki, Y. Zoka, and A. B. Khalifa Hussien, "A Novel Voltage Control Method for Distribution Systems based on P&Q Nodal Prices for Distributed Generations," *IEEJ Trans. Power Energy*, vol. 139, no. 3, pp. 178–185, Mar. 2019.

[44] N. Yorino, M. Danyoshi, and M. Kitagawa, "Interaction among multiple controls in tap change under load transformers," *IEEE Trans. Power Syst.*, vol. 12, no. 1, pp. 430–436, 1997.

Ahmed Bedawy (S'14) received the B.S. and M.Sc. degrees in Electrical Engineering from Aswan University, Aswan, Egypt, in 2007 and 2013, respectively. He is currently pursuing the Ph.D. degree at the Electric Power and Energy System Laboratory (EPESL), Graduate School of Engineering, Hiroshima University, Hiroshima, Japan. Since 2013, he has been an Assistant Lecturer with the Faculty of Engineering, South Valley University, Qena, Egypt. His research interests include Power Systems, Renewable Energy Sources, voltage control, Distributed Generation.

Naoto Yorino (M'91, SM'17) received B.S., M.S. and Ph. D degrees in Electrical Engineering from Waseda University, Japan, in 1981, 1983, and 1987, respectively. He joined R&D section Fuji Electric Co. Japan 1983- 1984. Since 1987, he has been at Hiroshima University, where he is a Professor from 2005, Vice Dean from 2009 to 2017. He was a Visiting Professor at McGill University, Canada 1991-1992, also a Visiting Professor at Hohai University, China 2014-2017. His activity includes Vice President, Power and Energy Society, IEE of Japan 2009-2011, Neutral member of the Rulemaking Committee, ESCJ 2007-2015, Steering Committee Member of Japan Power Academy 2012-2014, 2018-2019, Board of Director in iREP from 2007, Board of Director in IEIE of Japan from 2013-2019, and so on. He has authored/co-authored over 130 transaction papers in power and energy area.

Karar Mahmoud received the B.S. and M.Sc. degrees in electrical engineering from Aswan University, Aswan, Egypt, in 2008 and 2012, respectively. In 2016, he received the Ph.D. degree from the Electric Power and Energy System Laboratory (EPESL), Graduate School of Engineering, Hiroshima University, Hiroshima, Japan. Since 2010, he has been with Aswan University where he is presently Assistant Professor. Currently, he is a Postdoctoral Researcher at the School of Electrical Engineering, Aalto University, Finland. His research interests include Power Systems, Renewable Energy Sources, Smart Grids, Distributed Generation, and Optimization.

Yoshifumi Zoka (M'99) received B.S. degree in Electrical Engineering, M.S. and Ph.D. degrees in Systems Engineering from Hiroshima University, Japan. He is currently an Associate Professor in Graduate School of Engineering, Hiroshima University. He was a Research Associate at University of Washington, Seattle, WA, USA from 2002 to 2003. His research interest lies in power system planning, stability and control problems.

Yutaka Sasaki (M'08) received B.S., M.S. and Ph.D degree in Electrical Engineering from Hokkaido University, Japan in 2004, 2006, and 2008, respectively. He is an Assistant Professor at Hiroshima University. He was a Visiting Scholar at Washington State University, Pullman, WA, USA from 2012 to 2013. His research interests include optimal planning and operation of power system including renewable energy resources.